Separation Science and Technology
Publication details, including instructions for authors and subscription information:
http://www.informaworld.com/smpp/title~content=t713708471

Electrophoresis along a Semipermeable Membrane Surface

Joseph L. Shmidt[a]; Huk Y. Cheh[a]
[a] DEPARTMENT OF CHEMICAL ENGINEERING AND APPLIED CHEMISTRY, COLUMBIA UNIVERSITY, NEW YORK, NEW YORK

To cite this Article Shmidt, Joseph L. and Cheh, Huk Y.(1992) 'Electrophoresis along a Semipermeable Membrane Surface', Separation Science and Technology, 27: 1, 11 — 27
To link to this Article: DOI: 10.1080/01496399208018862
URL: http://dx.doi.org/10.1080/01496399208018862

SEPARATION SCIENCE AND TECHNOLOGY, **27**(1), pp. 11–27, 1992

Electrophoresis along a Semipermeable Membrane Surface

JOSEPH L. SHMIDT and HUK Y. CHEH
DEPARTMENT OF CHEMICAL ENGINEERING AND APPLIED CHEMISTRY
COLUMBIA UNIVERSITY
NEW YORK, NEW YORK 10027

Abstract

A new concept of electrophoretic fractionation along a semipermeable membrane boundary is presented. Batch electrophoresis along the membrane surface is investigated theoretically and experimentally as a basis for fractionating micron-sized particles. The charged particles are retained at the membrane surface from a buffer flow through the membrane. An electric field parallel to the membrane surface causes the particles to migrate along it. Experimental results are compared to theoretical predictions.

INTRODUCTION

All living systems perform electrophoretic exchange. There is a continuous transfer of ions, organic molecules, and macromolecules across cell membranes. Species diffuse toward specific sites on the membrane surface and across the lipid bilayer membrane. In many cases the diffusion toward the membrane surface and then along the surface toward specific sites on the cell membrane is believed to be aided by electrophoretic interactions. There is a three-dimensional electric field at the membrane surface. At present, only electrophoretic mass transfer across the membrane, either through the lipid bilayer or through the channels in the membrane proteins, has been investigated (*1*). Details of mass transfer along the membrane surface remain unknown. In this paper the electrophoretic migration of charged particles along synthetic membrane surfaces is investigated.

This work attempts to mimic electrophoretic mass transfer along the biological cell surface by establishing a membrane surface electrophoretic migration along the surface of a synthetic polymer membrane.

Current synthetic membranes are made from different polymers and their copolymers (*2*). These include cellulose, cellulose acetate, polysul-

fone, polypropylene, polyacrylonitrile, and polystyrene. The membranes come in a wide range of porosities, from reverse osmosis membranes with pore sizes of 5–10 Å, dialysis membranes of 10 to 30 Å, ultrafiltration membranes of 20 to 500 Å, to microfiltration membranes of 0.05 to 5 μm pores (*3*).

Most membranes are moderately hydrophilic (cellulose, cellulose acetate, sulfonated polysulfone) to highly hydrophilic (surface-modified polyacrylonitrile), or hydrophobic (polysulfone, polypropylene, polystyrene, polyacrylonitrile) (*4*). All membranes are either positively or negatively charged. The least charged membranes are made from regenerated cellulose or from surface-modified polyacrylonitrile.

Membrane surface electrophoresis (MSE) is considered as an alternative for analytical gel electrophoresis. The boundary layer at the membrane surface is used as an anticonvectant medium instead of the gel.

A typical gel electrophoresis comprises the electromigration of a small sample of a protein mixture through a slab of porous gel matrix. The gel is used to reduce thermal convection which arises from heat generated by the presence of an electric field. The gel also serves as a molecular sieve, retarding the motion of the larger species (*5*).

Although gel electrophoresis is a common technique for analyzing different macromolecules, it cannot be used to separate organelles and whole cells due to the restrictive gel sizing. Another difficulty is that a gel is not optically clear during fractionation (*6*).

Electrophoretic migration of charged particles along the membrane surface is investigated. The membrane is a thin porous film filled with a solvent but impermeable to the charged particles. The electric field parallel to the membrane surface drives the charged particles along the membrane, while the solvent flowing through the membrane keeps the particles at the porous membrane surface as shown in Fig. 1. As faster migrating particles get separated from the slower species, one is able to differentiate among them.

The sample size in membrane surface electrophoresis is small because fractionation occurs mainly in a microscopically thin layer on the membrane surface. Another advantage of membrane surface electrophoresis is that ultrafiltration and dialysis membranes can provide optically clear media, allowing simultaneous spectrophotometric detection. Finally, this technique favors separation of the larger cells with low diffusion coefficients without the restriction of gel sizing.

Modeling electrophoretic movement of charged species on semipermeable surfaces requires an understanding of the solute and solvent movement and their interactions with the membrane. Most studies on gel electrophoresis use a model involving the particle electrophoretic mobility in a free liquid environment with the incorporation of correction factors for

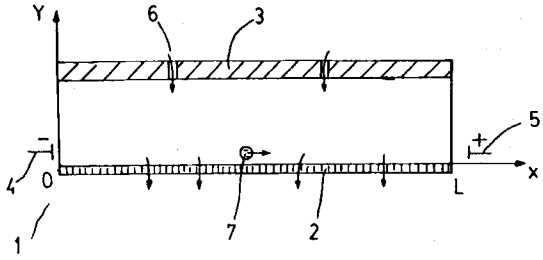

FIG. 1. A schematic drawing of the separation chamber. (1) Cross-sectional view of the horizontal cell, (2) a semipermeable membrane, (3) an upper plate, (4, 5) the cathode and the anode, (6) the inlet buffer flow into the fractionation chamber, (7) a negatively charged particle.

particle–matrix interactions. A fundamental understanding of gel electrophoresis is hindered by a lack of knowledge on the complexity of the electrostatic charge distribution and particle–matrix interactions in an electric field. For the most part, analytical gel electrophoresis is an empirical technique where electrophoretic mobility of the unknown species is compared to previously measured electrophoretic mobilities of well-known markers.

In our model, electrophoretic migration of charged species is combined with the electroosmotic buffer flow at the membrane surface. There are also effects due to the transmembrane pressure, membrane permeability, solute diffusion, heat dissipation, temperature and flow stability near the membrane surface, and adsorption and desorption of particles on the membrane.

THEORETICAL ANALYSIS

1. Concentration at the Membrane Surface

The electrophoresis of charged particles in a rectangular membrane chamber is shown schematically in Fig. 1. The width of the gap, h, between the membrane and the upper plate is much less than the length L, or the width of the membrane. Arrows across the membrane indicate continuous buffer flow (suction) through the membrane. The transmembrane flow is used to keep the charged species near the membrane surface and to stabilize the flow.

A significant factor for electrophoresis on the membrane surface is the dispersion of charged species as they migrate along the membrane. A higher dispersion rate results in poorer resolution.

If a small liquid sample containing charged particles is applied in a narrow

line to the membrane surface, the charged species will migrate along the surface, dispersing into wider bands with time. The liquid sample should be diluted sufficiently to prevent agglomeration of particles.

Neglecting the adsorption of particles to the membrane surface and thermal expansion, the concentration profile of particles is governed by

$$\frac{\partial c}{\partial t} + \mathbf{V}\cdot\nabla c + \mathbf{V}_{ep}\cdot\nabla c = D\nabla^2 c \tag{1}$$

where c is the solute concentration, $\mathbf{V}$ is the fluid velocity, $\mathbf{V}_{ep}$ is the electrophoretic migration velocity, and D is the diffusion coefficient. For a two-dimensional problem of solutes migrating along the membrane surface, Eq. (1) is reduced to Eq. (2) in scalar form:

$$\frac{\partial c}{\partial t} + (V_{eo} + V_{ep})\frac{\partial c}{\partial x} + J\frac{\partial c}{\partial y} = D\frac{\partial^2 c}{\partial y^2} + D\frac{\partial^2 c}{\partial x^2} \tag{2}$$

where V_{eo} is the flow parallel to the membrane surface, V_{ep} is the magnitude of the electrophoretic migration velocity, J is the magnitude of the velocity normal to the membrane, y is the distance normal to the membrane surface, and x is the distance along the membrane surface, as shown in Fig. 1.

a. Concentration Normal to the Membrane Surface

The concentration profile perpendicular to the membrane surface is established over a short time period (7). Therefore, as a first approximation, we assume that the concentration profile normal to the membrane surface at any given x coordinate is a function of y only and that it is not time dependent over small time intervals. Equation (1) simplifies to

$$\frac{\partial c}{\partial y} = \frac{D}{J}\frac{\partial^2 c}{\partial y^2} \tag{3}$$

Equation (3) is solved for a given flux J with boundary conditions, $c = c_0$ at $y = 0$; and $c = 0$ at $y \to \infty$.

$$c = c_0 \exp\left[-\frac{Jy}{D}\right] \tag{4}$$

Transmembrane permeation stabilizes the flow near the membrane surface. Flow stabilization by suction through the permeable boundary is a well-known method to prevent the onset of instabilities in boundary layers.

The determining factor is the ratio of the suction velocity to the velocity of the main flow. Even at relatively small values of these ratios, 10^{-3} to 10^{-5}, wall suction may prevent the onset of instability (*8*).

The migration of the species along the x axis is given by

$$\frac{\partial c}{\partial t} + V_e \frac{\partial c}{\partial x} = D \frac{\partial^2 c}{\partial x^2} \tag{5}$$

where V_e is the magnitude of the fluid velocity in the x direction, including both electrophoretic migration and electroosmotic flow, i.e., $V_e = V_{eo} + V_{ep}$.

b. Electroosmotic Flow

All solid surfaces acquire a charge when immersed into a liquid solution. Mechanisms through which surfaces may acquire a charge include preferential adsorption of ions, dissociation of surface groups, adsorption of polyelectrolytes, charged macromolecular species, and accumulation (or depletion) of electrons at the interface. These surface charges influence the charges distribution in the solution, because electroneutrality must be maintained in the system. An electrical double layer forms at the solid–solution interface.

In the electrical double layer, the charges on the surface are regarded as being stationary, while the induced opposite charges in the solution are mobile. When an electric potential is applied to the system, the mobile charges move toward an appropriate electrode and cause an electroosmotic flow. The velocity of these mobile charges depends upon a balance between the electrical driving force and the viscous drag force.

The electroosmotic flow near the membrane surface can be estimated from (*9*)

$$V_{eo} = \frac{\epsilon E \zeta}{4\pi\eta} - \frac{\epsilon E \psi_0}{4\pi\eta} \exp(-\kappa x) \tag{6}$$

Equation (6) is a first approximation for the electroosmotic flow along the membrane surface where ϵ is the dielectric constant, E is the electric field, η is the viscosity, ζ is the potential at the shear surface ($V = 0$), x is the distance from the surface, ψ_0 is the potential at the solid surface, and κ is the reciprocal of the Debye–Huckel double layer thickness (*10*, *11*).

In a closed chamber between two electrodes, electroosmotic flow occurs toward the electrodes. For a closed system, flow at the walls of the chamber must be compensated by a flow in the opposite direction near the center

(*12*). If the distance between the chamber walls and the particle size are both much larger than the double layer, velocity V_e can be assumed to be a constant, and

$$V_e = \frac{\epsilon \zeta}{4\pi\eta} + V_{ep} \tag{7}$$

c. *Concentration along the Membrane Surface*

By a change of variable from x to z where $z = x - V_e t$, we obtain a reference frame in which the zone center appears motionless, and Eq. (5) transforms to

$$\frac{\partial c}{\partial t} = D \frac{\partial^2 c}{\partial z^2} \tag{8}$$

The initial condition is an infinitely sharp band located at $x = 0$, i.e., at $z = 0$, $t = 0$, $c = w_0\delta(0)$, where $\delta(0)$ is the delta function and w_0 is the weight of solute in the band. The boundary conditions are

$$\text{at } z = 0, \qquad \partial c/\partial z = 0 \tag{9}$$

$$\text{at } z \to \infty, \qquad c = 0 \tag{10}$$

The solution to Eq. (8), subject to the initial and boundary conditions, is

$$c(x,t) = w_0/(4\pi Dt)^{1/2} \exp\left[-(x - V_e t)^2/4Dt\right] \tag{11}$$

Equation (11) predicts the spread of the solute band migrating electrophoretically on the membrane surface.

2. Temperature Field

The heat dissipated in the gap is removed by continuously recirculating a cooling electrolyte underneath the membrane. A horizontal chamber provides an additional flow stabilization from the temperature profile. The electrolyte temperature in the gap decreases toward the membrane surface, and the system is naturally stable. The Rayleigh instability factor is reversed (*13*). The temperature is calculated from the conservation of thermal energy at steady state:

$$C_v \mathbf{V}\cdot\nabla T + \nabla\cdot k\nabla T + \sigma E_0^2 = 0 \tag{12}$$

where C_v is the volumetric heat capacity, k is the thermal conductivity, σ is the electrical conductivity, $\mathbf{V}$ is the fluid velocity, and E_0 is the electric field strength.

For a narrow fractionation gap with negligibly small flow normal to the membrane surface, Eq. (12) is reduced to

$$k_i \frac{d^2T}{dy^2} + \sigma_i E^2 = 0, \qquad i = 1, 2 \tag{13}$$

where k_i is the thermal conductivity, with index 1 referring to the buffer electrolyte and index 2 referring to the buffer-filled membrane. Boundary conditions are as follows.

at $x = 0$:

$$k_i \left.\frac{dT}{dx}\right|_{x\to+0} = k_2 \left.\frac{dT}{dx}\right|_{x\to-0} \tag{14}$$

$$T|_{x\to+0} = T|_{x\to-0} \tag{15}$$

at $x = h$

$$dT/dx = 0 \tag{16}$$

at $x < -\delta$

$$T = T_0 \qquad \text{constant} \tag{17}$$

The solution of Eq. (13) subject to these boundary conditions is

$$T = -\frac{\sigma E^2}{k_1}\frac{y^2}{2} + \frac{\sigma E^2}{k_1} hy + \frac{\sigma E^2}{k_2} h\delta + T_0 \tag{18}$$

where h is the width of the gap and δ is the membrane thickness. Both the electrical and thermal conductivities are assumed to be constant.

3. Particle Adsorption in Membrane Surface Electrophoresis

Another important factor is the adsorption of particles to the membrane surface. Published data on pressure driven separations show that classical adsorption theory, e.g., the Langmuir isotherm, does not correspond well with experimental results. Adsorption of biomaterials in gel electrophoresis

is assumed to be negligible by gel manufacturers (*14*). According to recent experimental data on the kinetics of adsorption to the membrane surface, actual adsorption of cells does not occur for several minutes after the initial contact (*15*). On the other hand, membrane suction forces particles toward the membrane surface, increasing physical interactions.

Both the particle and the membrane surface are deformable. Therefore, if the particle "touches" the membrane surface, there is a finite contact area between them. Assuming that there is no seepage of the electrolyte solution underneath this area, the particle will be attached to the membrane surface with a force equal to the pressure differential across the membrane multiplied by the contact area.

Particle movement and adsorption to the membrane surface can be examined from a purely hydrodynamic consideration which discards diffusion. The analysis of flow around the particle can be summarized as a tangential flow of fluid parallel to the membrane, normal fluid flow to the membrane, and permeation flow through the membrane. The tangential flow of fluid parallel to the membrane is the electroosmotic flow. Fluid flow normal to the membrane is a transmembrane permeation flow J. Permeation flow through membrane pores is assumed to be uniform because the membrane pores are several orders of magnitude smaller than the charged particles. Goren (*16*) solved the resisting drag for a sphere "touching" a permeable membrane wall. Assuming that the particle and wall were in contact, he derived the force pushing the particle toward the membrane,

$$F_y = \phi 3\pi\eta d_p J \tag{19}$$

where d_p is the particle diameter, η is the fluid viscosity, and J is the transmembrane flow. Parameter ϕ is the wall correction factor of Stokes' law for the corresponding flow system. It can be estimated by (*17*)

$$\phi = \left[\frac{R_m d_p}{3} + (1.072)^2\right]^{1/2} \tag{20}$$

where R_m is the membrane resistance in units of cm^{-1}.

$$R_m = \Delta P/\eta J \tag{21}$$

where ΔP is the transmembrane pressure differential.

Electroosmotic flow along the membrane surface is given by Eq. (6). The force exerted on a single sphere touching the membrane wall by the

electroosmotic flow can be estimated by

$$F_{x,\text{drag}} = 0.75\epsilon E\zeta d_p \tag{22}$$

The electrophoretic force exerted on a charged particle by the electric field E is estimated from the free flow electrophoretic mobility of the same particle in the bulk solution:

$$F_{x,\text{el}} = 3\pi\eta d_p \mu_p E \tag{23}$$

where μ_p is the electrophoretic mobility of the particle in the bulk solution.

A sum of these two forces, F_x, is the force exerted on the particle in the x direction:

$$F_x = 3d_p E[\pi\eta\mu_p + 0.25\epsilon\zeta] \tag{24}$$

For a particle on an uneven surface of the membrane filter, the tangential force F_x tends to move particles along the membrane surface. The normal force F_y tends to entrain the particle as shown in Fig. 2a. A critical state is reached when these forces are in equilibrium. The moment of all forces about a contact point with the membrane is given by

$$M = 0.5d_p(F_x \cos\theta - F_y \sin\theta) \tag{25}$$

where θ is the angle of repose of the particle. The sign of the net moment will determine whether or not the sphere will move along the membrane surface. A positive value shows that the particle will migrate, and negative value shows that the particle will not move. When the moment is zero, Eq. (25) is reduced to

$$\theta_0 = \arctan \frac{E(\pi\eta\mu_p + 0.25\epsilon\zeta)}{\phi\pi\eta J} \tag{26}$$

where θ_0 is the angle of repose for the critical state. When the value of θ is smaller than θ_0, the particle will migrate along the membrane surface.

Angle θ has the physical interpretation as a quantitative parameter of all the interfacial forces between the particles and the membrane. As such, it is difficult to determine.

If there is a multilayer formation of particles on the membrane surface, a different value of the angle θ will need to be determined, as shown in Fig. 2b.

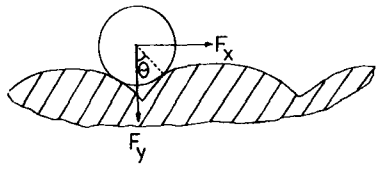

FIG. 2a. A schematic view of a particle on the uneven membrane surfaces.

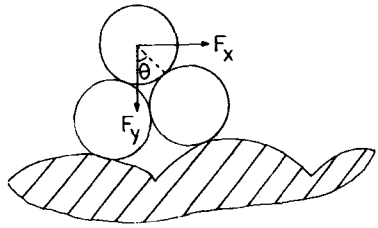

FIG. 2b. A schematic view of a multiparticle layer on the membrane surface.

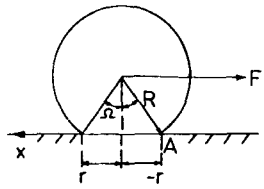

FIG. 2c. A schematic view of a contact area between the particle and the membrane surface.

For membrane surface electrophoresis of cells along the ultrafiltration or dialysis membranes, the membrane surface can be assumed to be relatively smooth compared to the size of the particle, as shown in Fig. 2c.

Because both the particle and the membrane surface are somewhat flexible, there is a finite contact area shown by a radius r in Fig. 2c. It is assumed that there is no seepage of the buffer electrolyte underneath this area. For the particle to migrate along the membrane surface, a rotating moment applied by the electrophoretic force F about a point A should exceed the moment from the pressure differential on the contact area πr^2, as shown in Fig. 2c.

$$FR \cos \Omega > 2 \int_{-r}^{r} (x + r)\Delta p(r^2 - x^2)^{1/2}\, dx \tag{27}$$

where Ω is the angle of contact, R is the radius of the particle, and Δp is the pressure differential across the membrane. Equation (27) is integrated and simplified for a small value of the contact angle Ω:

$$2\Delta p < \frac{F}{\pi R^2 \Omega^3} \tag{28}$$

At a critical state, the LHS and the RHS of Eq. (27) are equal and the critical contact angle is Ω_0:

$$\Omega_0 = \left(\frac{0.5F}{\pi \Delta p R^2}\right)^{1/3} \tag{29}$$

For example, a charged sphere with a 2-μm diameter and the electrophoretic mobility of 1 μm·cm/V·s at a 0.5 atmosphere pressure differential will have the critical contact angle of 0.9°. The radius of the contact area r will be equal to 155 Å.

EXPERIMENTAL

All experiments were carried out in the electrophoretic cell shown in Fig. 3, in which 1 was a hydrophilic regenerated cellulose 5000 molecular weight cut-off YM-5 membrane (Amicon Corp., Danvers, Massachusetts). Membrane 1 was placed between an upper clear polycarbonate plate 2 and a lower plate 3 made from high density polyethylene. The membrane edges were sealed with a rubber gasket 4. The electric field along the membrane surface was created between two platinum wire electrodes 5 and 6. The electrodes were placed into grooves 7 and 8 cut in plate 3. The distance between the electrodes was 15 cm. A pressurized buffer solution was supplied to the gap between membrane 1 and upper plate 2 through multiple inlets (not shown). Some of the buffer permeated through the membrane

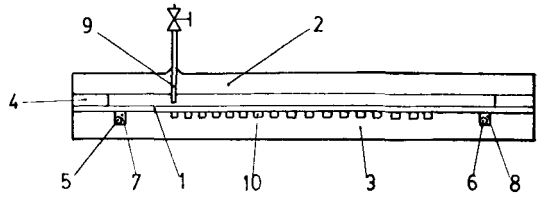

FIG. 3. Experimental cell. (1) A semipermeable membrane, (2) an upper clear plate, (3) a lower support plate, (4) a rubber gasket, (5, 6) the cathode and the anode, (7, 8) the electrode compartments, (9) a sample inlet needle, (10) a grid of grooves below the membrane.

into the grid of grooves 10 and flowed to the outside container. Two other separate electrolyte streams were recirculated by a peristaltic pump through the electrode compartments 7 and 8. The membrane 1 sealed around the edges of the electrode compartments from the pressure exerted by the electrolyte solution. A 0.02-mL drop of a 2 vol% mixture of particles was applied to the membrane surface in the form of a small circle through a 0.5-mm needle connected to a syringe with an ON/OFF valve.

In all experiments an electric field of approximately 11.6 V/cm was applied. The depth and width of the fractionation chamber were 0.15 and 3 cm, respectively. The electrolyte solution was recirculated through the electrode compartments at 12 mL/min. Temperature rise in the separation chamber was within 1.5°C after a 2-h experimental run.

Black latex beads (Seradyn Inc., Indianapolis, Indiana), 1.104 μm in diameter, and blue latex beads (Seradyn Inc.), 5.0 μm in diameter, were used. A Seamans buffer solution of pH 7.00 ± 0.05 (1.76 m*M* Na_2HPO_4, 0.367 m*M* KH_2PO_4, and 0.336 m*M* Na_2EDTA) was used in all experiments. Buffer conductivity was measured to be 0.002 ohm^{-1} cm^{-1}. Latex beads were suspended in the buffer and their electrophoretic mobilities were measured with a Model 1 Zeta-Meter (Zeta-Meter, Inc., New York, New York). The results were 4.2 ± 0.4 μm·cm/V·s for the negatively charged black beads and 0.2 μm·cm/V·s for the positively charged blue beads. A sample contained either 3×10^8 black beads or 3×10^6 blue beads.

During an experiment an electric field was generated between the electrodes with a constant voltage power supply from the Model 1 Zeta Meter. The sample was injected manually with a syringe onto the membrane surface, and its movement was visually monitored through the upper clear plate. Joule's electric heat was removed continuously by recirculating the buffer solution between the electrode compartments and an outside reservoir.

RESULTS AND DISCUSSION

The migration of the 1.1-μm diameter species was modeled by using Eq. (11). The diffusion coefficient was estimated from the Stokes–Einstein law to be 4×10^{-9} cm^2/s. The electrophoretic migration velocity was assumed to be 0.01 cm/s. Results of the calculations are shown in Fig. 4. A very small diffusional dispersion, approximately 0.02 cm, is predicted after 1000 s of electrophoresis.

The dispersion of species perpendicular to the membrane surface was calculated from Eq. (4), where flux J was equal to 0.6 μm/s. 99.99% of the particles remain within 7 μm from the membrane surface. Note that the electroosmotic velocity is practically constant within a few microns from the membrane surface.

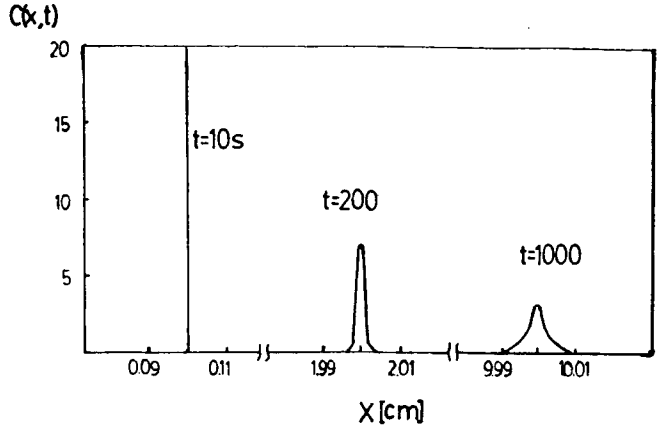

FIG. 4. Concentration profile of particles at different time intervals versus the distance migrated in the x direction.

The maximal temperature rise in the fractionation gap was calculated from Eq. (22) to be 0.2°C, where $k_1 = 0.006$ W/cm·°C, $k_2 = 0.003$ W/cm·°C, $\sigma = 0.002$ (ohm·cm)$^{-1}$, $h = 0.15$ cm, $\delta = 0.025$ cm, and $E = 11.6$ V/cm.

The experimental results are shown in Figs. 5 through 8.

Figure 5 shows electrophoretic migration of the black beads with time. The system geometry is also indicated on the Y-coordinate. The anode, cathode, and position of injection are at 12.4, −2, and 0 cm, respectively. The position of the beads is shown with a circle. Two circles connected by a bar represent a completely filled area of colored beads, with the upper and lower boundaries given by the upper and lower circles, respectively. All experiments started with a 1-cm diameter circle around the injection point. The experiment in Fig. 5 was done at 1 psi pressure with an average buffer flux of 0.6 μm/s. During the first 25 min, black beads migrated according to the theoretical prediction shown by the two dotted lines. Then some of the beads stopped migrating in the area between 6.2 and 7.2 cm. Other beads continued to move slowly until they reached the anode.

Another set of experimental results with the black beads is shown in Fig. 6. The transmembrane pressure was 10 psi with a transmembrane flux of 5.5 μm/s. All the beads migrated for a short period of time and then stopped in the area between 1.2 and 2.9 cm. It is obvious that the higher transmembrane pressure hinders the migration of the charged species, and leads to adsorption. According to Eq. (29), the critical contact angle Ω_0 is inversely proportional to the one-third power of the transmembrane pres-

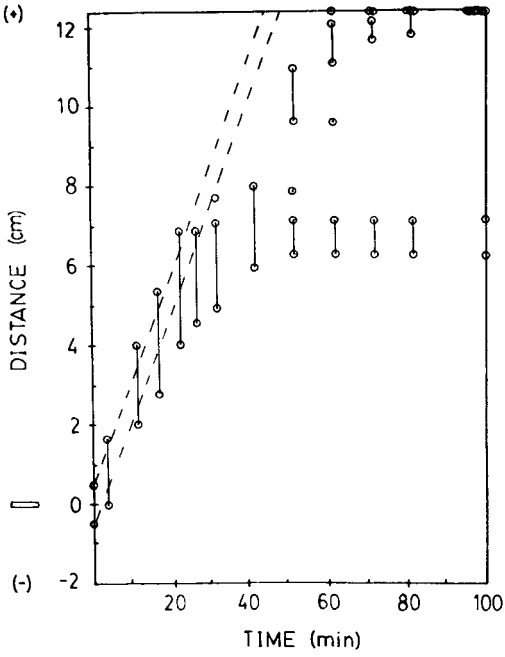

FIG. 5. Distance migrated by particles versus the time from the beginning of the experiment.

sure Δp; therefore, a larger transmembrane pressure leads to particle adsorption.

Figure 7 shows electrophoresis of the 5-μm positively charged latex beads at 0.6 μm/s transmembrane flow and 1 psi transmembrane pressure. An area of the blue beads is shown by two small filled circles connected by a bar. Blue beads did not show any electrophoresis and stayed within the same area where they were injected. Results of Eq. (29) are again in qualitative agreement with experimental results. Lower electrophoretic mobility and larger particle diameter correspond to the larger minimal value of the repose angle θ and lead to easier adsorption.

Fractionation of a mixture of the black and blue beads is shown in Fig. 8. The transmembrane flow was again 0.6 μm/s. A complete separation between the blue and the black beads was achieved, where the blue beads stayed within the same injection area and the black beads migrated toward the anode. A portion of the black beads traveled all the way to the anode, some were adsorbed in the area between 6.2 and 7.2 cm, and another group of black beads stopped migrating at 2 cm away from the injection point.

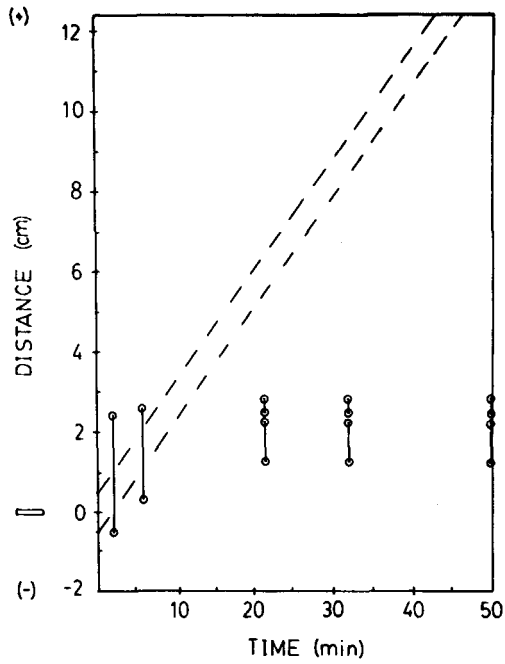

FIG. 6. Distance migrated by particles versus the time from the beginning of the experiment.

According to these results, it is possible to fractionate micron-size particles along the membrane surface. Particles stayed on the membrane surface within well-confined although scattered areas. There was no evidence of the three-dimensional dispersion typical for free flow electrophoresis methods. In practice, smoother and nonadsorbing membrane materials are required for improved separations.

CONCLUSIONS

A new electrophoretic method is proposed for the analytical fractionation of micron-sized particles. Membrane surface electrophoresis is expected to be a viable technique for fractionating small samples of cells and organelles.

Experimental results with charged latex beads on the cellulosic membrane surface indicate the importance of membrane–particle interactions and the transmembrane pressure on the particle adsorption. A smooth, hydrophilic, nonadsorbing membrane surface combined with a low trans-

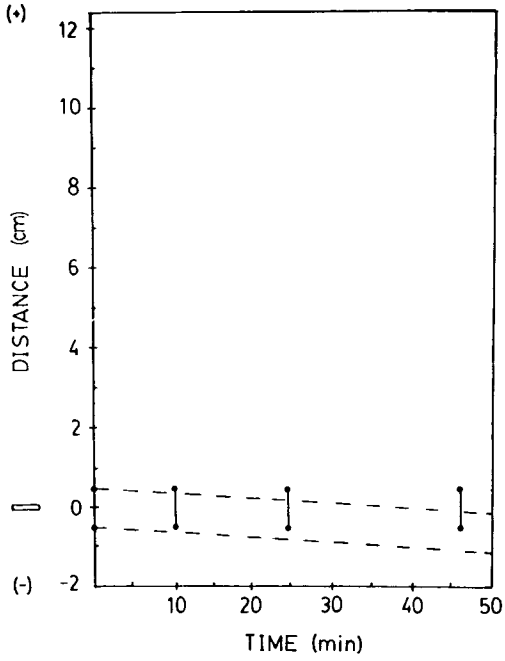

FIG. 7. Distance migrated by particles versus the time from the beginning of the experiment.

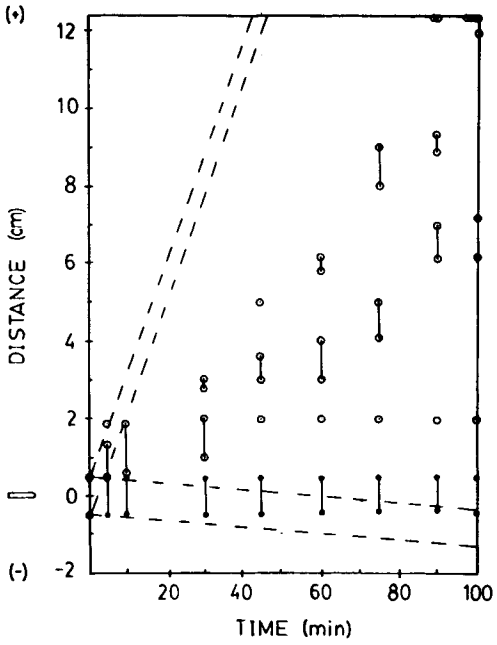

FIG. 8. Distance migrated by particles versus the time from the beginning of the experiment.

membrane pressure differential is required for fractionating a mixture of particles.

In addition to fractionating cells, membrane surface electrophoresis can probably be used to separate macromolecules, DNA and RNA strands, inorganic particles, and beads.

REFERENCES

1. A. S. Presman, *Electromagnetic Fields and Life,* Plenum Press, New York, 1970.
2. R. M. Quinn, *Desalination, 46,* 113 (1983).
3. J. Kassotis, J. Shmidt, L. Hodgins, and H. Gregor, *J. Membr. Sci., 22,* 61 (1985).
4. Products of Membrex, Inc., Garfield, New Jersey.
5. A. T. Andrews, *Electrophoresis,* Clarendon, Oxford, 1981.
6. Molecular Dynamics, *High Resolution Dynamic Imaging for Visualisation of Electrophoresis Gels,* Sunnyvale, California, 1989.
7. W. F. Blatt, A. Dravid, A. S. Michaels, and L. Nelson, in *Membrane Science and Technology* (J. E. Flinn, ed.), Plenum Press, New York, 1970, p. 47.
8. H. Schlichting, *Boundary Layer Theory,* McGraw-Hill, New York, 1979, p. 383.
9. J. Overbeek and B. Bijsterbasch, "The Electrical Double Layer and the Theory of Electrophoresis, in *Electrokinetic Separation Methods* (P. Rigetti, C. J. van Oss and J. M. Vanderhoff, eds.), Elsevier, Amsterdam, 1979, p. 1.
10. C. K. Lee, "Membrane Separation Coupled with Electrophoresis," PhD Thesis, Illinois Institute of Technology, 1987.
11. P. Hiemenz, *Principles of Colloid and Surface Chemistry,* Dekker, New York, 1977.
12. K. Hannig, *Electrophoresis, 3,* 235 (1982).
13. S. Chandrasekhar, *Hydrodynamic and Hydromagnetic Stability,* Dover, New York, 1961.
14. Pharmacia Fine Chemicals AB, *Gel Electrophoresis,* S-751 04 Uppsala 1, Sweden, 1982.
15. H. Flemming and G. Schaule, *Desalination, 70,* 95 (1988).
16. S. L. Goren, *J. Colloid Interface Sci., 23,* 1293 (1968).
17. W. M. Lu and S. C. Ju, *Sep. Sci. Technol., 24,* 517 (1989).

Received by editor February 26, 1990